ADVANCED ENGINEERING MATERIALS

COMMUNICATION

DOI: 10.1002/adem.201400209

Guiding and Deflecting Cracks in Bulk Metallic Glasses to Increase Damage Tolerance**

By *Jun Yi,* Wei Hua Wang* and *John J. Lewandowski*

Materials with high strength and toughness are desirable for lightweight and high-performance engineering structures.[1] Although bulk metallic glasses (BMGs) typically have the highest strength among bulk alloys,[2,3] the lack of tensile ductility and low toughness of some metallic glasses will limit their use in structural applications. Composition optimization has been used to develop tough BMG matrix composites and monolithic BMGs.[4–6] Ductile dendrites in BMG matrix composites can stabilize BMGs against the catastrophic fracture associated with extension of shear bands, producing graceful failure.[1,4–6] To design a tough BMG matrix composite, several criteria must be satisfied, otherwise the materials may become more brittle.[4] Robust theories that are able to predict new compositions that are able to satisfy so many different criteria are still unavailable. However, BMGs with high Poisson ratio (ν) appear to encourage multiple shear band formation at both notches and sharp cracks, thereby relieving local stress concentrations and producing an increase in toughness. This has become one criteria that has been used to search for tough(er) BMGs.[6–11] Recently, damage-tolerant $Ti_{40}Zr_{25}Cu_{12}Ni_3Be_{20}$ glass,[10] $Pd_{79}Ag_{3.5}P_6Si_{9.5}Ge_2$ glass,[8] and $Zr_{61}Ti_2Cu_{25}Al_{12}$ glass[12,13] were developed. Although the $Pd_{79}Ag_{3.5}P_6Si_{9.5}Ge_2$ glass has the same ν (0.42) as that of many other Pd- and Pt-based glasses, its toughness appears to be much higher.[7,8] However, sample size limitations and test details may contribute to inflated toughness numbers.[14] A scaling law has been developed that takes the cavitation activation barrier into account in order to predict the toughness of BMGs.[8] That work postulated that the toughness of metallic glasses should be proportional to ν and the glass transition temperature (T_g).[8] While this appears to explain the toughness of many BMGs,[8] neither $Ti_{40}Zr_{25}Cu_{12}Ni_3Be_{20}$ nor $Zr_{61}Ti_2Cu_{25}Al_{12}$ glass has a very high ν or high T_g, yet their fracture toughness values (i.e., notched and fatigue pre-cracked) are comparable to the highest toughness BMGs.[10,12] Thus, the intrinsic toughening mechanism that produce high toughness in monolithic BMGs is still unclear.

The present work utilizes pre-deformation of notched samples to significantly increase the notch toughness of both brittle and tough BMGs. This strategy utilizes pre-compression of notched components to locally change the deformation and fracture behavior in the vicinity of the notch, and results in significant increases to the notch toughness of both brittle and tough BMGs. In this aspect, toughening of various BMG components (e.g., screws, fillets, etc.) can be realized by changing the deformation/fracture behavior exactly where it is needed (e.g., at the tip of a stress concentration), rather than requiring predeformation of the whole sample or component. It is noted that there is much previous work[15–21] that has used cold rolling to improve the mechanical behavior of a variety of BMGs. However, these approaches may require very high loads on bulk samples (i.e., that are subsequently machined into components) due to the very high strengths of most BMGs. The novelty of the present work is that local deformation produced near a stress concentration (e.g., notch, fillet, threads, etc.) via simple pre-compression can be very effective in increasing the subsequent crack resistance of a component that contains a stress concentration. This work builds on very recent other work where this approach has also been shown to produce notch toughness increases under dynamic conditions.[21]

The approach developed presently somewhat mimics the toughening strategy that is effective in many natural biomineral materials. The excellent combination of strength and toughness of tooth tissues and mollusk shells[22,23] stems from the fact that these biological materials incorporate strong-yet-brittle minerals and soft organic phases with sophisticated micro-architectures.[1,23–26] The strong sub-micrometer building blocks provide strength while thin layers of soft organic phases encompass the mineral building blocks, maintaining integrity and dissipating energy during fracture.[1,4,23–26] Fundamental to the enhanced toughness of these natural materials is the ability to channel and deflect cracks through the soft organic phases.[1,25,26]

The present approach to increase the notch toughness of BMGs attempts to mimic these biological materials by creating other mechanisms of crack deflection. A brittle $Zr_{56}Co_{28}Al_{16}$ glass (ZC) and a tough $Zr_{61}Ti_2Cu_{25}Al_{12}$ glass (ZT) are chosen

[*] *Dr. J. Yi, Prof. J. J. Lewandowski*
Department of Materials Science and Engineering, Case Western Reserve University, 10900 Euclid Avenue, Cleveland, OH 44106, USA
E-mail: jxy305@gmail.com
Prof. W. H. Wang
Institute of Physics, Chinese Academy of Sciences, Beijing 100080, China

[**] *The financial support of this work was provided by ARO-W911NF-12-1-0022 with partial support from DTRA-1-11-1-0064. W.H.W. appreciates the financial support from NSF of China (51271195). The authors appreciate Chris Tuma (Advanced Manufacturing and Mechanical Reliability Center) for help in mechanical tests.*
Supporting Information is available from the Wiley Online Library or from the author.

ADVANCED ENGINEERING MATERIALS

here for investigation. The amorphous nature of as-cast BMGs and their relatively homogeneous structure precludes the possibility of such soft interfaces. However, shear bands in plastically deformed (and deforming) BMGs are softer than their surrounding regions[19,27–29] and the thickness of shear bands (about 10–20 nm[28,30]) is comparable to that of the soft organic phase in natural bio-mineral materials,[4] and much thinner than the soft phases in other bio-inspired materials, which are thicker than 1–2 μm.[24,25,31] The present strategy is to introduce pre-existing shear bands (PESBs) at a stress concentration to provide internal weak interfaces in a bulk material that will guide and deflect evolving cracks, thereby increasing the crack resistance. Deflection of cracking to regions that lie outside the plastic zone (i.e., of the original material) where the stresses are lower[32] should inhibit cavitation and further increase the toughness.[33] Although it is impossible for a crack to propagate out of the plastic zone of microscopically homogeneous as-cast BMGs, it is known that cracks in BMGs preferentially propagate along shear bands.[12,34] Therefore, if PESBs can be locally introduced into BMGs that exceed the plastic zone size of the original material, crack deflection beyond the plastic zone will be promoted.

The pre-compression method shown in Figure 1a was used to introduce PESBs into as-cast BMGs containing notches with a depth-to-width ratio of 0.45, introduced using a slow speed diamond wire saw with a diameter of 100 μm. The compressive fracture loads for ZT and ZC notch toughness samples are 13.6 and 23.3 kN, respectively (Supporting Information Figure S1a). However, unloading of identical notched samples prior to catastrophic fracture enabled production of PESBs emanating from the notch. Figure 1b shows PESBs in ZT that experienced a pre-compressive load P of only 12 kN. This approach can also be used to introduce PESBs into brittle BMGs such as ZC as shown in Supporting Information Figure S1b, although compressive loads higher than 9 kN will produce cracks in ZC during unloading, as shown in Supporting Information Figure S1c. As shown in Figure 1b and Supporting Information Figure S1b, the PESBs are locally arrested before penetrating through the sample. The plastic deformation that results from such pre-compression will eventually cause a reduction in notch root radius with increasing load P as shown in Supporting Information Figure S2. The size of the PESBs zone, R, measured as indicated by the arrow in Figure 1b increases with load P (Figure 2a). When $R > R_p$ (the plane stress plastic zone size) of the original material, the PESBs created will extend out of the plastic zone. Thus, the selection of a large enough pre-compressive load will create $R > R_p$, where $R_p = (K_c/\sigma_y)^2/(2\pi)$, K_c is the critical stress intensity factor, σ_y is the tensile yield strength. The R_p for notched samples of as-cast ZT and ZC are calculated to be 579 and 24 μm, respectively, based on known values for K_c and σ_y. The PESBs introduced in this manner are oriented closer to the direction that is normal to the nominal fracture plane than that exhibited by shear bands in the plastic zone of as-cast BMGs when R exceeds R_p. Furthermore, computer simulations show that cracks in tough(er) BMGs favor to initiation at 90° to the nominal fracture plane, and do so without cavitation.[33] Based on this background, we expect that PESBs properly introduced into BMGs will channel and deflect cracks in the manner analogous to that provided by the soft organic phases in

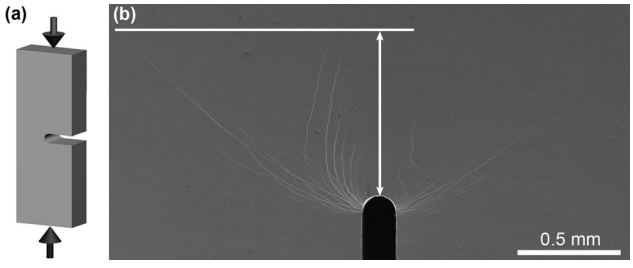

Fig. 1. Pre-compression of notched BMGs. (a) Schematic of the pre-compression of notched BMGs. The solid black arrows indicate the loading direction. (b) SEM image shows the PESBs introduced at the notch by pre-compression with a load of 12 kN. The PESBs zone size was measured in the manner indicated by the white arrow.

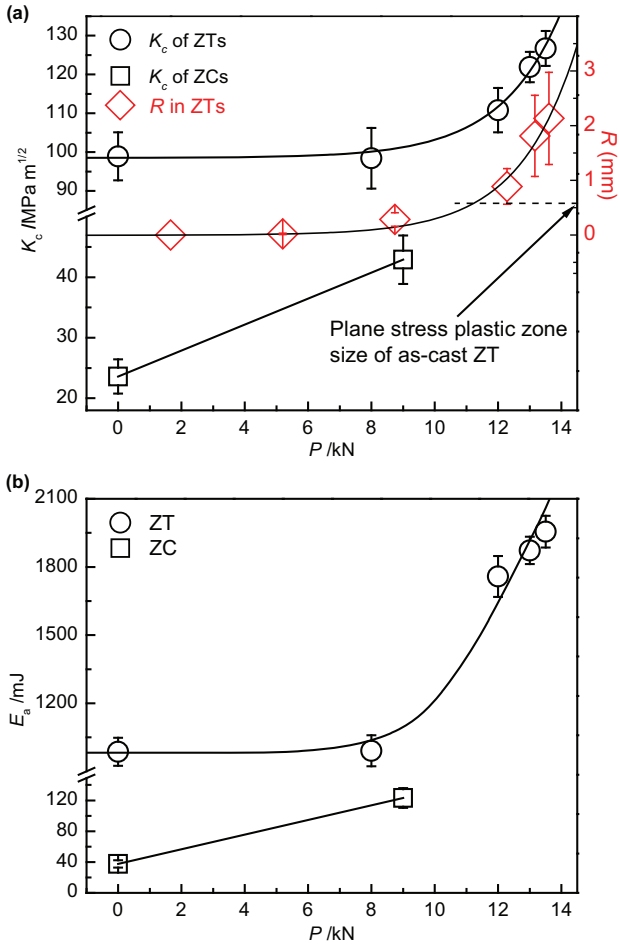

Fig. 2. Toughening of pre-compressed ZCs and ZTs. (a) PESBs zone size, R, increases with pre-compressive load P. When R is larger than plane-stress plastic zone size R_p of as-cast ZT, the notch toughness of ZT will be improved. R will exceed the plastic zone size of as-cast ZT at $P > 11$ kN. The notch toughness K_c of ZT was improved from 98.8 to 126.7 MPa m$^{1/2}$. Notch K_c of as-cast ZC was enhanced from 23.6 to 42.9 MPa m$^{1/2}$ at $P = 9$ kN. (b) The relationship between E_a and P of ZCs and ZTs are similar to K_c–P curve in (a). E_a of ZT and ZC were improved by 98 and 227%, respectively. The black solid lines are eyesight guide for data points. Error bars are standard deviation of five tests.

COMMUNICATION

bio-mineral materials. This should inhibit cavitation in the BMGs, producing elevated toughness.

The notch toughness of as-cast and pre-compressed ZCs and ZTs were measured and the results are shown in Figure 2. It is emphasized that the R must exceed the critical R_p of the as-cast sample before any enhancement of toughness is obtained in ZT, as shown in Figure 2a. Once this R_p (579 μm) is exceeded, the notched toughness (K_c) of ZT is improved from 98.8 to 126.7 MPa $m^{1/2}$. This approach also works for the more brittle ZC. Pre-compression of ZC with a load of 9 kN generates a PESBs zone with a size R of 173 μm (see Supporting Information Figure S1b), much larger than the R_p of the as-cast ZC (i.e., 24 μm). In this case, the notched K_c of ZC is increased from 23.6 to 42.9 MPa $m^{1/2}$. The improvements in notched K_c are consistent with other work showing that PESBs can enhance the ductility of BMGs.[19,34] In addition, the energy absorbed before catastrophic fracture, E_a, of ZCs and ZTs was calculated from the load–deflection curves of the three-point-bend notched toughness tests in the manner used by others.[24] The increase in E_a with load P exceeds the change of K_c with P, with improvements of E_a for ZTs and ZCs of 227 and 98%, respectively (Figure 2b). Bio-inspired materials[21–23,27] only showed an improvement in E_a due to such deflection. The present results demonstrate that pre-compression of notched samples can significantly enhance the fracture resistance of both brittle ZC and tough ZT for both crack initiation and growth, since both K_c and E_a are enhanced.

Scanning electron microscopy (SEM) was used to document the fracture surfaces in both plane-stress and plane-strain regions to confirm if crack deflection along PESBs and inhibition of cavitation was promoted by pre-compression. SEM images of the plane-stress regions in Figure 3 show the fracture behavior. Figure 3a shows a side view of the fractured as-cast ZT. It is clear that the crack in the as-cast tough ZT propagated along a shear band inside the plastic zone. In contrast, Figure 3b shows crack deflection beyond the as-cast plastic zone size ($R_p = (K_c/\sigma_y)^2/2\pi = 998$ μm) for ZT pre-compressed with a load of 13.5 kN. As shown in Figure 3c, cracking in the pre-compressed ZT was channeled and deflected into the outermost PESB. This is the closest shear band to the direction normal to the nominal fracture plane, as predicted by others.[33] Examination of failed samples reveals that the cracks locally arrest at PESB terminations. Such regions apparently force the crack to deviate to the second outermost PESB (Figure 3c). As shown in Figure 3d, the process of crack deflection from one PESB to another creates significant crack blunting via shear sliding.[33]

In contrast to the fracture behavior of ZT, fracture in as-cast ZC occurred in a more planar manner without shear banding (Figure 3e), consistent with its more brittle behavior. Such behavior suggests that the cavitation instability associated with the maximum hydrostatic stress $\sigma = \sigma_{ii}/3$ ahead of the crack tip[33] precedes shear banding in as-cast ZC. However, as shown by the black arrows in Figure 3f, cracking in ZC pre-compressed with a load of 9 kN deflects well beyond the plane stress plastic zone of as-cast ZC (i.e., $R_p = (K_c/\sigma_y)^2/2\pi = 87$ μm) under the guidance of the PESBs. It is clear that cracking in both ZC and ZT can be deflected beyond the as-cast plastic zone size by suitably introduced PESBs.

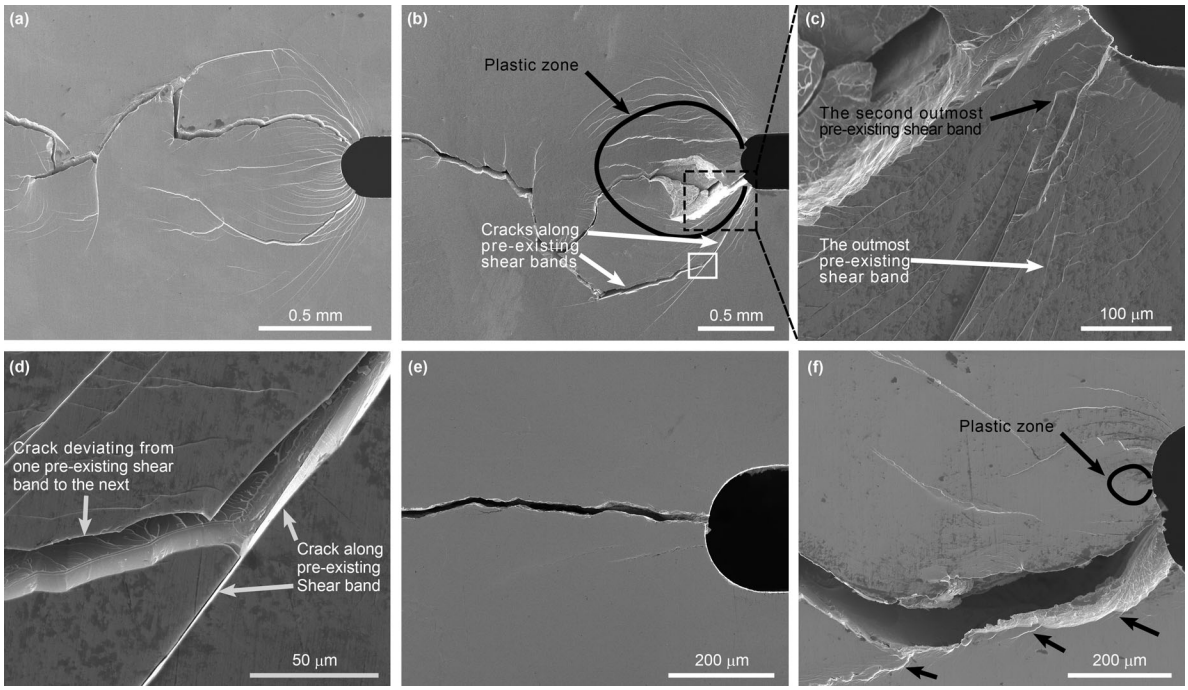

Fig. 3. SEM images illustrating crack deflection beyond the plastic zone along PESBs. (a) SEM image of side view of fractured as-cast ZT. (b) Side view of fractured ZT pre-compressed with a load of 13.5 kN. The crack deflected beyond the as-cast plastic zone under the guidance of PESBs. Details in the solid white rectangle are shown in (d). (c) The crack initiated at the outermost PESB. Then, the crack deviated to the second outermost PESB. (d) Crack deviation from one PESB to another. The crack blunted during crack deviation. (e) No shear band was found at the notch root of as-cast brittle ZC. (f) Fracture in ZC pre-compressed with a load of 9 kN was also deflected beyond the plastic zone under the guidance of PESBs, as indicated by the arrows. More extensive shear banding was noted in the pre-compressed ZC.

ADVANCED ENGINEERING MATERIALS

SEM observations in Figure 4 and Supporting Information Figure S5 provide insights into the mechanism(s) of toughening that may be operating in the plane-strain regions. In the plane-strain fractured regions of pre-compressed samples, "crack lips" and viscous fingering associated with strain-controlled continuous crack opening[34–36] along shear bands were observed. In these cases, crack lips are different from shear lips,[37] which are associated with shear sliding. The crack-lip size at the crack initiation locations in ZC and ZT pre-compressed to 9 and 13.5 kN, respectively, are measured to be 142 and 410 μm, respectively (see Supporting Information Figure S3b and e). The plane-strain plastic zone sizes r_p of the pre-compressed ZC and ZT are calculated ($r_p = (K_c/\sigma_y)^2/6\pi$) to be 29 and 332 μm, respectively, and are much smaller than the crack lips. This confirms that the crack in the plane-strain region also deflects beyond the plastic zone along PESBs.

Dimple-like (i.e., cavitation) features on the fracture surface of the as-cast ZT (Figure 4a and Supporting Information Figure S3a) were absent on the fracture surface of the ZT pre-compressed with a load of 13.5 kN, Figure 4b and Supporting Information Figure S3b. Instead, the pre-compressed ZT exhibited smooth and featureless shear-sliding zones, pits with viscous fingering, crack lips. Matching fracture surface features on the pre-compressed ZT are shown in Supporting Information Figure S4. The smooth featureless shear-sliding zones are indicative of crack-tip blunting during crack propagation,[38] while dimple-like features indicate stress-assisted cavitation and linking of voids ahead of the crack tip.[36,38] In contrast, viscous fingering is associated with a strain-controlled meniscus instability and continuous crack opening.[35,36] Even though strain-controlled continuous fracture has been reported in the plane stress regions of fractured human cortical bone,[39] metallic glassy ribbons,[34] and microscale metallic glassy wires,[40] it has not been reported in plane strain regions.

Although pre-compression of tough ZT completely eliminated cavitation, pre-compression of ZC with a load of 9 kN did not totally suppress cavitation in ZC. Nevertheless, a crack lip (Supporting Information Figure S3e) with viscous fingering (Supporting Information Figure S3f) at crack initiation was observed in ZC while the length of the dimple-like region increased from 1.5 mm (Supporting Information Figure S3d) in as-cast ZC to 2.0 mm (Supporting Information Figure S3e) in the pre-compressed ZC. Furthermore, although the dimple size is not unique as shown in Figure 4c and d, its average value increased from 670 nm in as-cast ZC to 870 nm in the pre-compressed ZC. Finally, no cavitation was observed in the plane stress region of either pre-compressed ZC or ZT, as shown in Supporting Information Figure S5.

In summary, the notch toughness of both brittle ZC and tough ZT were improved by introducing architectured PESBs to both deflect cracks and inhibit cavitation. This effect occurs despite the accompanying decrease in notch radius (Supporting Information Figure S2), which has been shown to reduce the toughness of as-cast BMGs.[6,41,42] Although the combination of yield strength and toughness of as-cast ZT is among the best materials known,[12] its notch toughness was further improved significantly. The success of this toughening strategy requires that the PESBs extend beyond the original plastic zone of the as-cast BMGs, since the crack cannot be deflected outside of plastic zone otherwise. It is necessary that the PESBs produced by pre-compression are arrested. These PESBs can arrest and blunt a propagating crack by forcing the crack to transfer from one PESB to another. This strategy appears particularly promising for components containing stress concentrations where local PESBs can be introduced as this will not require plastic deformation of the whole material/structure. However, additional investigations may achieve even higher toughness by optimizing such approaches.

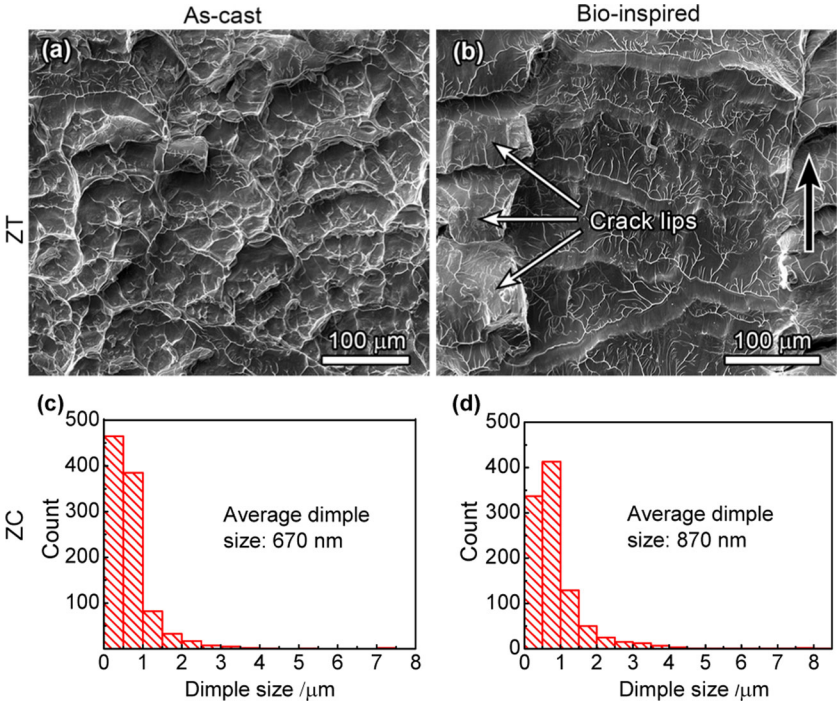

Fig. 4. Transformation of microscopic fracture patterns on the fracture surfaces of as-cast and pre-compressed ZTs and ZCs. (a) Dimple-like features on the fracture surface of as-cast ZT. (b) Smooth and featureless shear-sliding zones, pits with viscous fingering, crack lips, and deflected cracks under crack lips present on plane strain regions of the fracture surface of ZT pre-compressed with a load of 13.5 kN. The black arrow indicates crack-propagation direction. Statistics of dimple size on fracture surface of as-cast (c) and pre-compressed (with a load of 9 KN) ZC (d). The average dimple sizes of as-cast and the pre-compressed ZC are 670 and 870 nm, respectively.

1. Experimental

1.1. BMG Plate Production

ZT and ZC plates were prepared by arc melting elemental pieces with purity higher

than 99.9 wt% and subsequent suction casting under a Ti-gettered argon atmosphere in a vacuum chamber. The fully amorphous nature of the plates was confirmed by X-ray diffractometer (Scintag X-1) and differential scanning calorimeter (Perkin-Elmer DSC-7).

1.2. Test Sample Preparation

As-cast samples were carefully cut and ground for pre-compression and subsequent notch toughness test in order to avoid effects of sample size limitations and test details as described in literature.[43] Bars with lengths of about 26.5 mm were cut from the bottom of as-cast plates with dimensions of $3.3 \times 8.1 \times 60$ mm using a low-speed diamond blade saw. The side surfaces of the samples were ground using 240, 400, 600, 800, and 1200 grit SiC papers. Error of thickness, width, and sample length of every sample were within 10 μm. Therefore, the opposite faces of the sample were parallel to each other. In order to keep neighboring faces of the samples perpendicular to each other, the samples were examined using orthogonal cross-marks in an optical microscope during grinding. The final dimensions of the ground bars are $3 \times 6 \times 26$ mm. The single edge notches were introduced using a slow speed diamond wire saw with a diameter of 100 μm to a depth of 2.7 mm.

1.3. Pre-Compression and Notch Toughness Test

Pre-compression shown in Figure 1a was conducted using an MTS Model 810 servo-hydraulic testing machine under displacement control at a rate of $0.09\,\mathrm{mm\,min^{-1}}$. The opposing edges of the notch remained parallel to each other after pre-compression, since the compressed faces of the samples were parallel as were the compression anvils. Three-point-bend notch fracture toughness tests were conducted similar to other work in the literature[11] on an Instron 1361 electromechanical test machine with a span of 24 mm under displacement control at a rate of $0.3\,\mathrm{mm\,min^{-1}}$ at room temperature. To confirm the reproducibility of the experimental results, five samples were tested for each data point.

1.4. SEM Imaging

The fracture surface and shear bands were investigated using Quanta 200 scanning electron microscope.

Received: April 30, 2014
Revised: August 4, 2014
Published online: September 3, 2014

[1] R. O. Ritchie, *Nat. Mater.* **2011**, *10*, 817.
[2] R. T. Qu, Z. F. Zhang, *Sci. Rep.* **2013**, *3*, 1117.
[3] A. Inoue, B. Shen, H. Koshiba, H. Kato, A. R. Yavari, *Nat. Mater.* **2003**, *2*, 661.
[4] D. C. Hofmann, J. Y. Suh, A. Wiest, M. L. Lind, M. D. Demetriou, W. L. Johnson, *Proc. Natl. Acad. Sci. USA* **2008**, *105*, 20136.
[5] D. C. Hofmann, J. Y. Suh, A. Wiest, G. Duan, M. L. Lind, M. D. Demetriou, W. L. Johnson, *Nature* **2008**, *451*, 1085.
[6] J. J. Lewandowski, M. Shazly, A. Shamimi Nouri, *Scr. Mater.* **2006**, *54*, 337.
[7] J. Schroers, W. L. Johnson, *Phys. Rev. Lett.* **2004**, *93*, 255506.
[8] M. D. Demetriou, M. E. Launey, G. Garrett, J. P. Schramm, D. C. Hofmann, W. L. Johnson, R. O. Ritchie, *Nat. Mater.* **2011**, *10*, 123.
[9] S. V. Madge, D. V. Louzguine-Luzgin, J. J. Lewandowski, A. L. Greer, *Acta Mater.* **2012**, *60*, 4800.
[10] X. J. Gu, S. J. Poon, G. J. Shiflet, J. J. Lewandowski, *Acta Mater.* **2010**, *58*, 1708.
[11] J. J. Lewandowski, X. J. Gu, A. S. Nouri, S. J. Poon, G. J. Shiflet, *Appl. Phys. Lett.* **2008**, *92*, 09.
[12] Q. He, J. K. Shang, E. Ma, J. Xu, *Acta Mater.* **2012**, *60*, 4940.
[13] Q. He, Y. Q. Cheng, E. Ma, J. Xu, *Acta Mater.* **2011**, *59*, 202.
[14] J. J. Lewandowski, *Philos. Mag.* **2013**, *93*, 3893.
[15] Y. Yokoyama, K. Yamano, K. Fukaura, H. Sunada, A. Inoue, *Mater. Trans.* **2001**, *42*, 623.
[16] J. S. Park, H. K. Lim, J. H. Kim, J. M. Park, W. T. Kim, D. H. Kim, *J. Mater. Sci.* **2005**, *40*.
[17] M. H. Lee, J. Das, K. S. Lee, U. Kühn, J. Eckert, *Intermetallics* **2010**, *18*, 1902.
[18] M. H. Lee, K. S. Lee, J. Das, J. Thomas, U. Kühn, J. Eckert, *Scr. Mater.* **2010**, *62*, 678.
[19] Y. Zhang, W. H. Wang, A. L. Greer, *Nat. Mater.* **2006**, *5*, 857.
[20] H. B. Yu, J. Hu, X. X. Xia, B. A. Sun, X. X. Li, W. H. Wang, H. Y. Bai, *Scr. Mater.* **2009**, *61*, 640.
[21] G. Sunny, V. Prakash, J. Lewandowski, *Metall. Mater. Trans. A* **2013**, *44*, 4644.
[22] H. Gao, B. Ji, I. L. Jäger, E. Arzt, P. Fratzl, *Proc. Natl. Acad. Sci. USA* **2003**, *100*, 5597.
[23] J. D. Currey, J. D. Taylor, *J. Zool.* **1974**, *173*, 395.
[24] G. Mayer, *Science* **2005**, *310*, 1144.
[25] M. Mirkhalaf, A. K. Dastjerdi, F. Barthelat, *Nat. Commun.* **2014**, *5*, 3166.
[26] P. Y. Chen, J. McKittrick, M. A. Meyers, *Prog. Mater. Sci.* **2012**, *57*, 1492.
[27] J. Bokeloh, S. V. Divinski, G. Reglitz, G. Wilde, *Phys. Rev. Lett.* **2011**, *107*, 235503.
[28] A. L. Greer, Y. Q. Cheng, E. Ma, *Mater. Sci. Eng. R* **2013**, *74*, 71.
[29] J. J. Lewandowski, A. L. Greer, *Nat. Mater.* **2006**, *5*, 15.
[30] D. Klaumünzer, A. Lazarev, R. Maaß, F. H. Dalla Torre, A. Vinogradov, J. F. Löffler, *Phys. Rev. Lett.* **2011**, *107*, 185502.
[31] E. Munch, M. E. Launey, D. H. Alsem, E. Saiz, A. P. Tomsia, R. O. Ritchie, *Science* **2008**, *322*, 1516.
[32] J. R. Rice, in *Fracture: An Advanced Treatise*, Vol. 2, (Eds: H. Liebowitz), Academic Press, New York **1968**, Ch. 3.
[33] P. Murali, T. F. Guo, Y. W. Zhang, R. Narasimhan, Y. Li, H. J. Gao, *Phys. Rev. Lett.* **2011**, *107*, 215501.

ADVANCED ENGINEERING MATERIALS

[34] H. J. Leamy, T. T. Wang, H. S. Chen, *Metall. Trans.* **1972**, *3*, 699.
[35] A. S. Argon, M. Salama, *Mater. Sci. Eng.* **1976**, *23*, 219.
[36] X. X. Xia, W. H. Wang, *Small* **2012**, *8*, 1197.
[37] G. R. Garrett, M. D. Demetriou, J. Chen, W. L. Johnson, *Appl. Phys. Lett.* **2012**, *101*, 241913.
[38] A. Tatschl, C. J. Gilbert, V. Schroeder, R. Pippan, R. O. Ritchie, *J. Mater. Res.* **2000**, *15*, 898.
[39] R. K. Nalla, J. H. Kinney, R. O. Ritchie, *Nat. Mater.* **2003**, *2*, 164.
[40] B. Zberg, E. R. Arata, P. J. Uggowitzer, J. F. Löffler, *Acta Mater.* **2009**, *57*, 3223.
[41] P. Lowhaphandu, J. J. Lewandowski, *Scr. Mater.* **1998**, *38*, 1811.
[42] J. J. Lewandowski, *Mater. Trans.* **2001**, *42*, 633.
[43] B. Gludovatz, S. E. Naleway, R. O. Ritchie, J. J. Kruzic, *Acta Mater.* **2014**, *70*, 198.

